

# Effect of H<sub>2</sub> reduction on the catalytic properties of MoO<sub>3</sub> with noble metals for the conversions of pentane and propan-2-ol

Takeshi Matsuda,\* Shuhei Uozumi and Nobuo Takahashi

Department of Materials Science, Kitami Institute of Technology, 165 Koen-cho, Kitami, Hokkaido 090-8507, Japan. E-mail: matsutk@mail.kitami-it.ac.jp; Fax: +81 157 26 4973; Tel: +81 157 26 9448

Received 15th August 2003, Accepted 26th November 2003  
First published as an Advance Article on the web 12th January 2004

The catalytic properties of H<sub>2</sub>-reduced MoO<sub>3</sub> with noble metals for the conversions of pentane and propan-2-ol were studied. No appreciable difference appeared in the pentane isomerization activity and in the propan-2-ol dehydration activity among Pt, Pd, Rh, and Ir/MoO<sub>3</sub> catalysts after reduction at 773 K for 12 h. H<sub>2</sub>-Reduced Ru/MoO<sub>3</sub> exhibited lower isomerization and dehydration activities than the other catalysts. The isomerization and the dehydration activities of H<sub>2</sub>-reduced Ru/MoO<sub>3</sub> was improved by an increase in the amount of Ru loading, while those of H<sub>2</sub>-reduced Pt/MoO<sub>3</sub> changed very little. XRD and TPR studies showed that the reduction process of Ru/MoO<sub>3</sub> varied with the amount of Ru. By contrast, reduction of Pt/MoO<sub>3</sub> involved the formation of a hydrogen molybdenum bronze, H<sub>x</sub>MoO<sub>3</sub>, irrespective of the amount of Pt. We suggest from these results that reduction of H<sub>x</sub>MoO<sub>3</sub> can yield the active phase for pentane isomerization and for propan-2-ol dehydration.

## Introduction

Hydrocarbon upgrading processes such as reforming, hydrocracking, isomerization, and catalytic iso-dewaxing play important roles in the hydrocarbon processing industry. In these processes, hydrocarbon molecules are cracked, aromatized and/or isomerized. Boosting the octane quality of a gasoline fraction by increasing the degree of branching of alkanes is an environmentally more acceptable alternative compared with other technologies such as blending with oxygenates and aromatics. Thus, skeletal isomerization of alkanes has attracted much attention as a reaction to produce clean fuels with high octane quality. Bifunctional catalysts containing both acid and metal functions have shown high efficiency in the isomerization of alkanes. The isomerization of pentane and hexane has successfully been carried out using Pt/chlorinated Al<sub>2</sub>O<sub>3</sub>, Pt/zeolites, and Pt/SO<sub>4</sub><sup>2-</sup>-ZrO<sub>2</sub> catalysts.

Iglesia and co-workers<sup>1-4</sup> reported that WC modified by chemisorbed oxygen catalyzed alkane isomerization without excessive cracking. They have suggested a traditional bifunctional mechanism on the oxygen modified WC, dehydrogenation-hydrogenation reactions on sites with a metallic character (WC<sub>x</sub>) and C-C bond rearrangement reactions on acid sites (WO<sub>x</sub>). Ledoux and co-workers have proposed that alkane isomerization reactions on oxygen-modified Mo<sub>2</sub>C and carbon-modified MoO<sub>3</sub> proceeded through a metallocyclobutane intermediate-based mechanism.<sup>5-8</sup> Molybdenum oxycarbide, MoO<sub>x</sub>C<sub>y</sub>, which is formed by incorporating carbon atoms in the molybdenum oxide lattice, has been considered to be the active phase for alkane isomerization.<sup>9,10</sup>

We showed in previous papers<sup>11-14</sup> that H<sub>2</sub> reduction of MoO<sub>3</sub> at 623 K yielded an active and selective catalyst for heptane isomerization, and its activity was dependent on the extent of reduction. H<sub>2</sub>-Reduced MoO<sub>3</sub> catalyzed the dehydrogenation and the dehydration of propan-2-ol simultaneously. We have suggested on the basis of these experimental results that the isomerization of heptane on H<sub>2</sub>-reduced MoO<sub>3</sub> can proceed *via* a conventional bifunctional mechanism. Maire

and co-workers have also proposed a traditional bifunctional mechanism on MoO<sub>2</sub>.<sup>15</sup> Loading of noble metals onto MoO<sub>3</sub> was reported to improve the catalytic activities for both heptane isomerization and propan-2-ol dehydration.<sup>16-18</sup> The isomerization and dehydration activities of H<sub>2</sub>-reduced Pt/MoO<sub>3</sub> were dependent on the extent of reduction, and the highest activities appeared at a reduction degree of about 70%. We reported in a previous paper<sup>19</sup> that H<sub>2</sub>-reduced Pt/MoO<sub>3</sub> exhibited high isomerization activity only when reduction of Pt/MoO<sub>3</sub> involved the formation of the hydrogen molybdenum bronze, H<sub>x</sub>MoO<sub>3</sub>. However, the role of Pt in the generation of the active phase for alkane isomerization is still under investigation. The aim of the present work is to describe the effects of loading of noble metals on the catalytic behaviors of H<sub>2</sub>-reduced MoO<sub>3</sub> for the conversions of pentane and propan-2-ol.

## Experimental

### Materials

H<sub>2</sub> and He were purified by passage through molecular sieves and a Mn/SiO<sub>2</sub> oxygen trap. H<sub>2</sub>MoO<sub>4</sub> of purity 98% was purchased from Kanto Chemical Co. Inc. Commercially available noble metal chlorides, H<sub>2</sub>PtCl<sub>6</sub>·6H<sub>2</sub>O, PdCl<sub>2</sub>, RhCl<sub>3</sub>·3H<sub>2</sub>O, RuCl<sub>3</sub>·*n*H<sub>2</sub>O and IrCl<sub>4</sub>·*n*H<sub>2</sub>O, were used without further purification. Pentane and propan-2-ol of purity 99.3 and 99.5%, respectively, were dried using molecular sieves prior to use. The MoO<sub>3</sub> used in this study was obtained by calcination of H<sub>2</sub>MoO<sub>4</sub> at 673 K for 3 h. Noble metal-loaded MoO<sub>3</sub> catalysts were prepared by a conventional impregnation method using an aqueous solution of noble metal chloride. Pt, Pd, Rh and Ir/MoO<sub>3</sub> were dried overnight at 393 K, and then were calcined at 673 K for 3 h. Since the formation of gaseous RuO<sub>4</sub> leads to loss of Ru, Ru/MoO<sub>3</sub> was treated at 673 K for 3 h in a stream of N<sub>2</sub>. The catalyst powders were compressed into flakes, followed by crushing and sieving (30–60 mesh).

## Reduction procedures

Noble metal-loaded MoO<sub>3</sub> catalysts weighing 0.2 g were packed at the central position of a cell, which was made of a Pyrex glass tube with an inner diameter of 8 mm. The sample was heated to 773 K at a rate of 5 K min<sup>-1</sup> in a stream of H<sub>2</sub>, and then was kept at that temperature for 12 h. Our previous papers showed that the physical and catalytic properties of MoO<sub>3</sub> with and without Pt changed depending on the flow rate of H<sub>2</sub> in the reduction process.<sup>20–22</sup> Hence, the reduction was performed at a fixed H<sub>2</sub> flow rate of 30 ml min<sup>-1</sup> in this study.

## Catalytic tests

Reaction of pentane was carried out at 523 K under atmospheric pressure in a conventional fixed bed flow reactor equipped with a sampling valve for gas chromatographic analysis. After H<sub>2</sub> reduction and cooling to reaction temperature in a stream of H<sub>2</sub>, pentane was introduced onto the catalyst bed at a partial pressure of 9211 Pa with H<sub>2</sub> as a complement to atmospheric pressure. Reaction of propan-2-ol was performed at 398 K and at a molar He/2-propanol ratio of 20. The composition of effluent gases was analyzed by FID gas chromatography using a TC-1 glass capillary separation column, and using a Porapak Q separation column.

## Characterization methods

The surface area was determined from an N<sub>2</sub> adsorption isotherm, which was obtained on the sample without exposure to air. The reduced sample was cooled to room temperature under H<sub>2</sub> flow. After evacuation for 0.5 h at room temperature, adsorption of N<sub>2</sub> was measured at 77 K with a conventional high-vacuum static system.

The extent of reduction was calculated from the amounts of O<sub>2</sub> consumed in the reoxidation that was performed at 773 K by a pulse technique. Since H<sub>2</sub>O was formed in the reoxidation, the concentration of O<sub>2</sub> was monitored with TCD gas chromatography using a Porapak N separation column. In this study, reduction of MoO<sub>3</sub> to Mo metal is defined to be a reduction degree of 100%.

Crystalline phases of the H<sub>2</sub>-reduced sample were determined by X-ray diffraction (XRD) using Ni-filtered Cu-K $\alpha$  radiation (Rigaku, Rint-1000). The sample for XRD measurements was obtained as follows: noble metal-loaded MoO<sub>3</sub> was reduced under set conditions, followed by flowing N<sub>2</sub> for 0.5 h. After cooling to room temperature under N<sub>2</sub> flow, the reduced sample was transferred to a glove box without exposure to air, and was dispersed in a solution of heptane to avoid any bulk oxidation.

Temperature-programmed reduction (TPR) was carried out to investigate the reducibility of noble metal-loaded MoO<sub>3</sub>. A sample weighing 0.4 g was treated at 673 K for 1 h in a stream of Ar, and then was cooled to room temperature. Ar was replaced by a H<sub>2</sub>-Ar gas mixture with 20% or 50% H<sub>2</sub>, followed by heating to 1098 K at a rate of 5 K min<sup>-1</sup>. The concentrations of H<sub>2</sub> and H<sub>2</sub>O were monitored with TCD gas chromatography using a Porapak N separation column at 413 K.

## Results and discussion

Conversion of pentane was carried out at 523 K under atmospheric pressure using noble metal-loaded MoO<sub>3</sub> catalysts. Here, the catalysts were reduced at 773 K for 12 h. The activities of the H<sub>2</sub>-reduced catalysts for the conversion of pentane declined very slightly with time on stream: under the reaction conditions employed, the conversion level of pentane over H<sub>2</sub>-reduced 0.01 mol% Pt/MoO<sub>3</sub> after a 1 h run was 15.1%, and was lowered to 14.0% after a 6 h run. The degree of

catalyst deactivation was independent of the noble metal and of the amounts of noble metal loading. Hence, the catalytic activity was estimated using data taken after a 1 h run. The physical and the catalytic properties of H<sub>2</sub>-reduced MoO<sub>3</sub> with noble metal are summarized in Table 1. All of the catalysts exhibited a reduction degree of about 80%. No appreciable difference appeared in the pentane isomerization activity among Pt, Pd, Rh, and Ir/MoO<sub>3</sub> catalysts. H<sub>2</sub>-reduced Ru/MoO<sub>3</sub> exhibited a lower isomerization activity than other catalysts, although the isomerization selectivity changed very little with the noble metal used. Since the surface area of H<sub>2</sub>-reduced Ru/MoO<sub>3</sub> was small compared with those of other catalysts, the pentane isomerization activity was evaluated by taking the surface area into consideration. As shown in Table 1, the smaller surface area of H<sub>2</sub>-reduced Ru/MoO<sub>3</sub> was not responsible for its lower isomerization activity.

Alkane isomerization has been considered to proceed *via* a bifunctional mechanism, a C<sub>5</sub>-ring hydrogenolysis process, or a metallocyclobutane bond-shift mechanism. Ledoux and co-workers<sup>5–8</sup> proposed that molybdenum oxycarbide catalyzed the isomerization of alkanes through a metallocyclobutane bond-shift mechanism. Maire and co-workers<sup>15</sup> reported that the MoO<sub>2</sub> phase was able to catalyze the isomerization of alkanes. They have suggested, from the results of systematic studies using catalytic reactions in association with spectroscopic techniques, that the isomerization reaction on MoO<sub>2</sub> proceeded *via* a bifunctional mechanism. Dehydrogenation and hydrogenation reactions might occur on the metallic sites represented by a certain density of state of the free valence electrons localized along the *c*-axis of a rutile deformed lattice. Electronegative oxygen might act as an acid site by fixing dissociated hydrogen produced on the metallic sites, thus providing Brønsted acid sites. Recently, Meunier has reported that a bifunctional mechanism operated in the isomerization of butane over H<sub>2</sub>-reduced MoO<sub>3</sub> and the rate-determining step may be the isomerization of an *n*-butene intermediate to isobutene.<sup>23</sup> We showed in previous papers<sup>13,18</sup> that H<sub>2</sub>-reduced MoO<sub>3</sub> and Pt/MoO<sub>3</sub> were active for both the dehydration and the dehydrogenation of propan-2-ol, indicating the presence of dual sites. H<sub>2</sub>-Reduced MoO<sub>3</sub> and Pt/MoO<sub>3</sub> provided negative reaction orders toward H<sub>2</sub> in pentane and heptane isomerization.<sup>24,25</sup> This behavior is a characteristic of alkane isomerization on bifunctional catalysts, such as Pt/zeolite. We have suggested from these experimental results that H<sub>2</sub>-reduced Pt/MoO<sub>3</sub> can catalyze alkane isomerization through the conventional bifunctional mechanism.

To study the bifunctional properties of noble metal-loaded MoO<sub>3</sub> samples, reaction of propan-2-ol was carried out at 398 K. Typical results are summarized in Table 2, where the catalytic activities were compared using data after a 0.5 h run to minimize the effect of catalyst deactivation. Here, the catalysts reduced at 773 K for 12 h were employed. Propan-2-ol was dehydrated to propene and diisopropyl ether (DIPE),

**Table 1** Catalytic activity of H<sub>2</sub>-reduced noble metal-MoO<sub>3</sub> samples for the conversion of pentane

Noble metal <sup>a</sup>	Reduction degree <sup>b</sup> (%)	Surface area/m <sup>2</sup> g <sup>-1</sup>	Conversion <sup>c</sup> (%)	Isomerization selectivity (%)	Rate of isomerization/10 <sup>-5</sup> mol h <sup>-1</sup> m <sup>-2</sup>
Pt	78.8	272	15.1	99.7	5.5
Pd	80.6	279	15.0	99.7	5.3
Rh	77.5	288	12.9	99.7	4.3
Ir	80.1	270	12.3	99.7	4.6
Ru	82.3	212	5.6	99.3	2.7

<sup>a</sup> 0.01 mol%. <sup>b</sup> Reduction conditions, 773 K 12 h. <sup>c</sup> Reaction conditions: temperature, 523 K; catalyst weight, 0.2 g; flow rate of pentane, 2.0 × 10<sup>-2</sup> mol h<sup>-1</sup>; H<sub>2</sub>/pentane, 10 (molar ratio).

**Table 2** Catalytic activity of H<sub>2</sub>-reduced noble metal-MoO<sub>3</sub> samples for the conversion of propan-2-ol

Noble metal	Conversion <sup>a</sup> (%)	Formation rate/mol h <sup>-1</sup> g <sup>-1</sup>			Ratio of formation rate: <i>R</i> <sub>propene</sub> / <i>R</i> <sub>acetone</sub>
		Propene	Diisopropyl ether	Acetone	
Pt	24.7	3.5 × 10 <sup>-2</sup>	6.5 × 10 <sup>-3</sup>	1.6 × 10 <sup>-3</sup>	22
Pd	25.2	3.6 × 10 <sup>-2</sup>	6.9 × 10 <sup>-3</sup>	5.7 × 10 <sup>-4</sup>	63
Rh	23.4	3.4 × 10 <sup>-2</sup>	6.2 × 10 <sup>-3</sup>	4.8 × 10 <sup>-4</sup>	71
Ir	22.9	3.4 × 10 <sup>-2</sup>	5.5 × 10 <sup>-3</sup>	7.2 × 10 <sup>-4</sup>	47
Ru	11.8	1.7 × 10 <sup>-2</sup>	3.1 × 10 <sup>-3</sup>	5.5 × 10 <sup>-4</sup>	31

The amounts of noble metal loading and reduction conditions: see Table 1. <sup>a</sup> Reaction conditions: temperature, 398 K; catalyst weight, 0.1 g; flow rate of propan-2-ol, 2.0 × 10<sup>-2</sup> mol/h; He/propan-2-ol, 20 (molar ratio).

and was dehydrogenated to acetone. All of the catalysts yielded propene much more selectively by dehydration relative to DIPE. No appreciable difference appeared in the dehydration activity among H<sub>2</sub>-reduced Pt, Pd, Rh and Ir/MoO<sub>3</sub> catalysts. H<sub>2</sub>-Reduced Ru/MoO<sub>3</sub> exhibited a lower dehydration activity than the other catalysts. The highest dehydrogenation activity was obtained on H<sub>2</sub>-reduced Pt/MoO<sub>3</sub>. H<sub>2</sub>-Reduced Pd, Rh, Ir and Ru/MoO<sub>3</sub> catalysts provided almost comparable dehydrogenation activity. We deduce from these results that the isomerization activity of H<sub>2</sub>-reduced MoO<sub>3</sub> with noble metals can be controlled by the acidity. The lower isomerization activity of H<sub>2</sub>-reduced Ru/MoO<sub>3</sub> is likely to result from its lower ability to act as an acid catalyst.

Table 3 shows the physical and catalytic properties of H<sub>2</sub>-reduced MoO<sub>3</sub> with the different amounts of Pt and Ru. In the case of H<sub>2</sub>-reduced Pt/MoO<sub>3</sub>, the reduction degree, the surface area, and the pentane isomerization activity depended little on the amounts of Pt loading. By contrast, the pentane isomerization activity of H<sub>2</sub>-reduced Ru/MoO<sub>3</sub> was improved by an increase in the amount of Ru loading. The isomerization activities of the catalysts with 0.05 and 0.1 mol% Ru were comparable to those of H<sub>2</sub>-reduced Pt/MoO<sub>3</sub>. The amount of Ru-loading had effects on the surface area and the reduction degree as well as on the isomerization activity. The surface area increased and the reduction degree decreased with increasing amount of Ru. 0.005 mol% Ru/MoO<sub>3</sub> showed the largest reduction degree and the smallest surface area among the catalysts tested after reduction at 773 K for 12 h. We showed in previous papers<sup>13,18</sup> that the alkane isomerization activity of H<sub>2</sub>-reduced MoO<sub>3</sub> with and without Pt was strongly affected by the extent of reduction. Hence, the isomerization activity was compared at a reduction degree of about 80%. A reduction degree of 82% was obtained in 0.005 mol% Ru/MoO<sub>3</sub> after reduction at 773 K for 6 h. As expected from the previous results, the surface area and the isomerization

activity were improved by a decrease in the reduction degree. However, the isomerization activity of the above sample was much lower than those of the catalysts with a larger amount of Ru.

Reaction of propan-2-ol was conducted to evaluate the bifunctional properties of H<sub>2</sub>-reduced MoO<sub>3</sub> with the different amounts of Pt and Ru. Typical results are shown in Table 4. The dehydrogenation reaction on H<sub>2</sub>-reduced Pt/MoO<sub>3</sub> was promoted by an increase in the amount of Pt, while the dehydration activity did not change at all. In the case of H<sub>2</sub>-reduced Ru/MoO<sub>3</sub>, the dehydration activity was enlarged and the dehydrogenation activity was lowered by an increase in the amount of Ru loading. A decrease in the reduction degree seems to lower the dehydrogenation activity. No appreciable difference appeared in the dehydration activity between 0.001 and 0.1 mol% Pt/MoO<sub>3</sub> and 0.1 mol% Ru/MoO<sub>3</sub>. When the dehydration activity was compared at a reduction degree of about 80%, H<sub>2</sub>-reduced 0.005 mol% Ru/MoO<sub>3</sub> exhibited the lowest dehydration activity among the catalysts tested. Since the dependency of the dehydration activity on the amounts of Pt and Ru loading was very similar to that of the isomerization activity, we suggest that the isomerization activity of H<sub>2</sub>-reduced MoO<sub>3</sub> with noble metals can be determined by the ability to act as an acid catalyst.

Fig. 1 illustrates the XRD patterns of Pt/MoO<sub>3</sub> reduced at 773 K for 12 h. The XRD pattern did not change at all with the amount of Pt. The diffraction lines appeared at 2θ = 38.1, 40.7 and 44.3°. The line at 40.7° is assigned to the *d*(110) plane of Mo metal. The diffraction lines at 2θ = 38.1 and 44.3° are considered to reflect the formation of a molybdenum oxyhydride phase, MoO<sub>x</sub>H<sub>y</sub>, according to the literature.<sup>12,18</sup> As shown in Fig. 2, Ru/MoO<sub>3</sub> reduced at 773 K for 12 h was also a mixture of the MoO<sub>x</sub>H<sub>y</sub> and Mo metal phase, irrespective of the amount of Ru. However, the intensity of the line at 40.7° was strengthened by a decrease in the amount of Ru, indicating that the formation of Mo metal was promoted in the presence of a smaller amount of Ru. This phenomenon is consistent with the results shown in Table 3: The extent of reduction was increased by a decrease in the amount of Ru. 0.005 mol% Ru/MoO<sub>3</sub> reduced at 773 K for 6 h, of which the reduction degree was 82%, consisted of MoO<sub>2</sub>, MoO<sub>x</sub>H<sub>y</sub> and Mo metal phases. By contrast, no diffraction line due to the MoO<sub>2</sub> phase was observed in 0.1 mol% Ru/MoO<sub>3</sub> and 0.001–0.1 mol% Pt/MoO<sub>3</sub>, which were reduced at 773 K for 12 h and their reduction degrees were 78–80%.

To study the reduction process of MoO<sub>3</sub> in the presence of Pt and Ru, changes in the XRD patterns during heating to 773 K in a stream of H<sub>2</sub> were measured. The sample was kept at room temperature for 0.5 h in an H<sub>2</sub> flow, followed by heating to a desired temperature and then quenching. The XRD patterns of 0.005 mol% Ru/MoO<sub>3</sub> are depicted in Fig. 3. 0.005 mol% Ru/MoO<sub>3</sub> heated to 473 K consisted of a hydrogen molybdenum bronze, H<sub>0.34</sub>MoO<sub>3</sub> and the MoO<sub>3</sub> phases, although the bulk was mostly the MoO<sub>3</sub> phase. The intensity of the lines due to the H<sub>0.34</sub>MoO<sub>3</sub> phase was strengthened at

**Table 3** Catalytic activities of H<sub>2</sub>-reduced Pt/MoO<sub>3</sub> and Ru/MoO<sub>3</sub> for the conversion of pentane

Noble metal	Amount (mol%)	Reduction degree (%)	Surface area/m <sup>2</sup> g <sup>-1</sup>	Conversion <sup>b</sup> (%)	Rate of isomerization/mol h <sup>-1</sup> m <sup>-2</sup>
Pt	0.001	79.4	280	8.9	5.4 × 10 <sup>-5</sup>
	0.01	78.8	272	9.6	5.9 × 10 <sup>-5</sup>
	0.1	80.3	277	11.9	6.9 × 10 <sup>-5</sup>
Ru	0.005	98.0	55	0.02	6.7 × 10 <sup>-7</sup>
	0.01	82.3	212	4.7	3.6 × 10 <sup>-5</sup>
	0.05	78.0	275	10.1	6.1 × 10 <sup>-5</sup>
	0.1	78.3	280	10.0	6.1 × 10 <sup>-5</sup>
	0.005 <sup>a</sup>	81.6	152	0.4	3.6 × 10 <sup>-6</sup>

Catalysts were reduced at 773 K for 12 h. <sup>a</sup> Catalyst was reduced at 773 K for 6 h. <sup>b</sup> Reaction conditions: temperature, 523 K; catalyst weight, 0.2 g; flow rate of pentane, 3.3 × 10<sup>-2</sup> mol h<sup>-1</sup>.

**Table 4** Catalytic activities of H<sub>2</sub>-reduced Pt/MoO<sub>3</sub> and Ru/MoO<sub>3</sub> for the conversion of propan-2-ol

Noble metal	Amount (mol%)	Conversion <sup>b</sup> (%)	Formation rate/mol h <sup>-1</sup> g <sup>-1</sup>			Ratio of formation rate: $R_{\text{propene}}/R_{\text{acetone}}$
			Propene	Diisopropyl ether	Acetone	
Pt	0.001	26.6	$3.9 \times 10^{-2}$	$6.7 \times 10^{-3}$	$6.5 \times 10^{-4}$	60
	0.01	24.7	$3.5 \times 10^{-2}$	$6.5 \times 10^{-3}$	$1.6 \times 10^{-3}$	22
	0.1	29.8	$3.6 \times 10^{-2}$	$7.8 \times 10^{-3}$	$7.9 \times 10^{-3}$	5
Ru	0.005	3.3	$3.1 \times 10^{-3}$	$1.2 \times 10^{-3}$	$1.1 \times 10^{-3}$	28
	0.01	11.8	$1.7 \times 10^{-2}$	$3.1 \times 10^{-3}$	$5.5 \times 10^{-4}$	31
	0.05	16.4	$2.6 \times 10^{-2}$	$3.4 \times 10^{-3}$	$2.0 \times 10^{-4}$	130
	0.1	19.7	$3.0 \times 10^{-2}$	$4.1 \times 10^{-3}$	$1.6 \times 10^{-4}$	187
	0.005 <sup>a</sup>	10.2	$1.3 \times 10^{-2}$	$2.6 \times 10^{-3}$	$1.7 \times 10^{-3}$	8

Reduction conditions: see Table 3. <sup>a</sup> Reduced at 773 K for 6 h. <sup>b</sup> Reaction conditions: see Table 2.

573 K. The diffraction lines due to the H<sub>0.34</sub>MoO<sub>3</sub> phase disappeared, and MoO<sub>2</sub> was formed at 673 K. 0.005 mol% Ru/MoO<sub>3</sub> gave the diffraction lines only due to the MoO<sub>2</sub> phase after heating to 773 K. The MoO<sub>2</sub> phase was also detected by XRD in 0.01 mol% Ru/MoO<sub>3</sub> after heating to 673 K and above, although the formation of H<sub>0.34</sub>MoO<sub>3</sub> was promoted. 0.01 mol% Ru/MoO<sub>3</sub> heated to 773 K in an H<sub>2</sub> flow was a mixture of the MoO<sub>2</sub> and the MoO<sub>x</sub>H<sub>y</sub> phases. When compared at a reduction degree of about 80%, H<sub>2</sub>-reduced 0.01 mol% Ru/MoO<sub>3</sub> gave no MoO<sub>2</sub>, while the MoO<sub>2</sub> phase was observed in H<sub>2</sub>-reduced 0.005 mol% Ru/MoO<sub>3</sub> (Fig. 2). This implies that the amount of MoO<sub>2</sub> formed in 0.01 mol% Ru/MoO<sub>3</sub> was smaller than that in 0.005 mol% Ru/MoO<sub>3</sub>.

Fig. 4 shows the XRD diagrams of 0.1 mol% Ru/MoO<sub>3</sub> heated to 298–773 K in a stream of H<sub>2</sub>. The formation of H<sub>0.34</sub>MoO<sub>3</sub> was detected at 373 K. When heated to 473 K, the MoO<sub>3</sub> phase disappeared completely, and hydrogen molybdenum phases, H<sub>0.93</sub>MoO<sub>3</sub> and H<sub>1.64</sub>MoO<sub>3</sub>, were formed. 0.1 mol% Ru/MoO<sub>3</sub> heated to 573 K and above gave no diffraction lines due to the hydrogen molybdenum bronze phases, and was almost amorphous with respect to XRD. As shown in Fig. 5, the H<sub>0.34</sub>MoO<sub>3</sub> and the H<sub>0.93</sub>MoO<sub>3</sub> phases were detected in 0.001 mol% Pt/MoO<sub>3</sub> at room temperature, indicating the high ability of Pt to activate hydrogen. These phases were converted to the H<sub>1.68</sub>MoO<sub>3</sub> phase at 473 K. No

appreciable difference appeared in the XRD pattern between 0.001 mol% Pt/MoO<sub>3</sub> and 0.1 mol% Ru/MoO<sub>3</sub> when they were heated to 573 K and above. 0.1 mol% Pt/MoO<sub>3</sub> provided almost the same results as 0.1 mol% Ru/MoO<sub>3</sub> and 0.001 mol% Pt/MoO<sub>3</sub>, although 0.1 mol% Pt/MoO<sub>3</sub> was converted to H<sub>1.68</sub>MoO<sub>3</sub> at room temperature. These results indicate that 0.001–0.1 mol% Pt/MoO<sub>3</sub> and 0.1 mol% Ru/MoO<sub>3</sub> were reduced through the hydrogen molybdenum bronze phases without the formation of MoO<sub>2</sub>. By contrast, reduction of 0.005 and 0.01 mol% Ru/MoO<sub>3</sub> was accompanied by the formation of MoO<sub>2</sub>, probably due to its low activity for hydrogen activation, although a part of the MoO<sub>3</sub> phase was converted to H<sub>0.34</sub>MoO<sub>3</sub>.

Temperature-programmed reduction (TPR) was performed to evaluate the reduction process of Pt and Ru/MoO<sub>3</sub>. Fig. 6 shows the profiles of H<sub>2</sub> consumption and of H<sub>2</sub>O formation during TPR of Pt/MoO<sub>3</sub> in a 20% H<sub>2</sub>–80% Ar gas mixture. 0.001 mol% Pt/MoO<sub>3</sub> reacted with H<sub>2</sub> without an equivalent amount of water being generated in the region of 298–495 K,

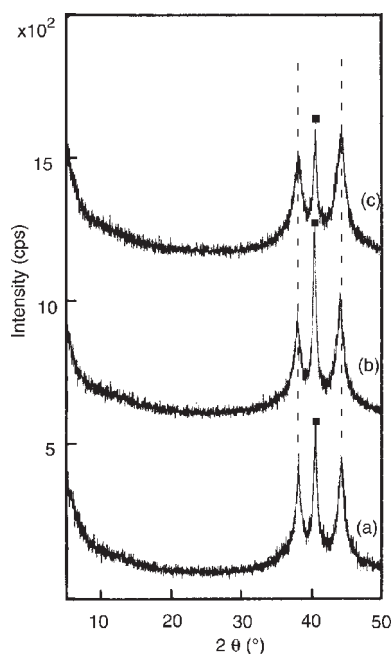


**Fig. 1** XRD Patterns of Pt/MoO<sub>3</sub> reduced at 773 K for 12 h. Pt loading (mol%): (a) 0.1, (b) 0.01, (c) 0.001; Mo metal (■).

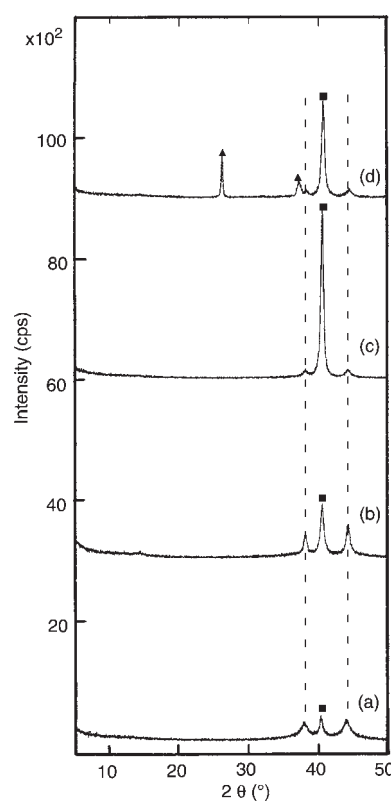


**Fig. 2** XRD Patterns of Ru/MoO<sub>3</sub>. Ru loading (mol%): (a) 0.1, (b) 0.01, (c) 0.005, (d) 0.005; (a), (b), (c) were reduced at 773 K for 12 h; (d) was reduced at 773 K for 6 h; MoO<sub>2</sub> (▲), Mo metal (■).

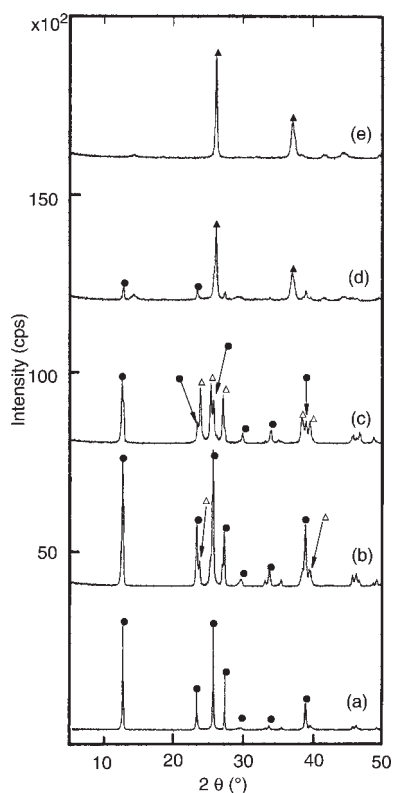


**Fig. 3** Change in the XRD patterns of 0.005 mol% Ru/MoO<sub>3</sub> during heating in an H<sub>2</sub> flow. (a) Room temperature, (b) 473 K, (c) 573 K, (d) 673 K, (e) 773 K: MoO<sub>3</sub> (●), MoO<sub>2</sub> (▲), H<sub>0.34</sub>MoO<sub>3</sub> (Δ).

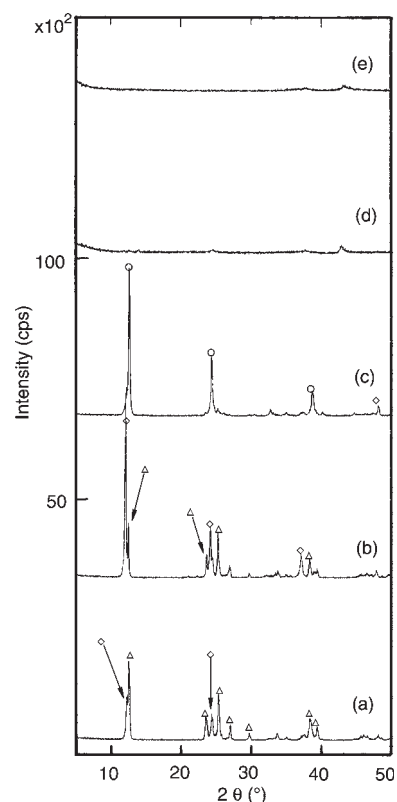


**Fig. 5** Change in the XRD patterns of 0.001 mol% Pt/MoO<sub>3</sub> during heating in an H<sub>2</sub> flow. (a) Room temperature, (b) 373 K, (c) 473 K, (d) 573 K, (e) 773 K: H<sub>0.34</sub>MoO<sub>3</sub> (Δ), H<sub>0.93</sub>MoO<sub>3</sub> (◇), H<sub>1.68</sub>MoO<sub>3</sub> (○).

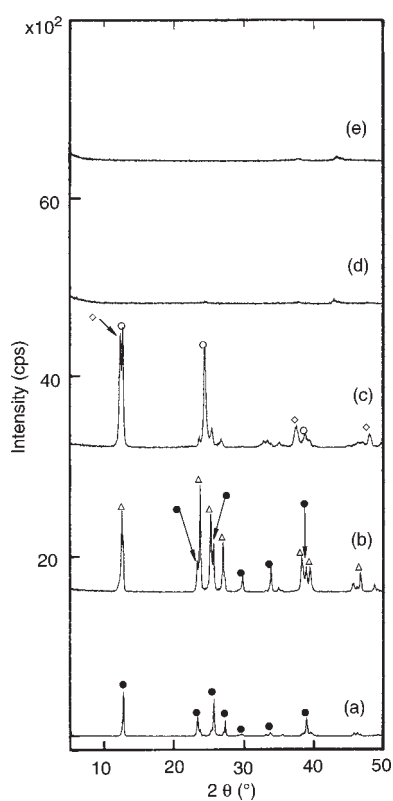


**Fig. 4** Change in the XRD patterns of 0.1 mol% Ru/MoO<sub>3</sub> during heating in an H<sub>2</sub> flow. (a) Room temperature, (b) 373 K, (c) 473 K, (d) 573 K, (e) 773 K: MoO<sub>3</sub> (●), H<sub>0.34</sub>MoO<sub>3</sub> (Δ), H<sub>0.93</sub>MoO<sub>3</sub> (◇), H<sub>1.68</sub>MoO<sub>3</sub> (○).

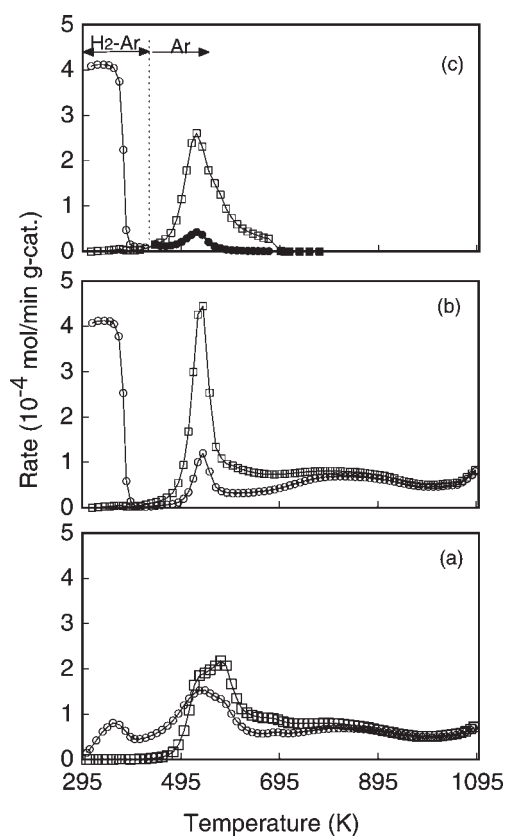


**Fig. 6** TPR spectra of 0.001 mol% Pt/MoO<sub>3</sub> (a) and 0.01 mol% Pt/MoO<sub>3</sub> (b, c). Conditions: sample weight, 0.4 g; gas, 20% H<sub>2</sub>-Ar (a, b), Ar (c); flow rate, 20 ml min<sup>-1</sup>; heating rate, 5 K min<sup>-1</sup>; H<sub>2</sub> consumption (○), H<sub>2</sub> formation (●), H<sub>2</sub>O formation (□).

indicating the formation of the  $H_xMoO_3$  phase. This phenomenon can be understood by hydrogen spillover.  $H_2O$  was formed with consuming  $H_2$  in the middle temperature range of 495–695 K, although large amounts of  $H_2O$  were evolved compared with the amounts of  $H_2$  reacted. No appreciable difference appeared between the amounts of  $H_2O$  formed and those of  $H_2$  consumed at temperatures above 795 K. 0.01 mol% Pt/ $MoO_3$  consumed large amounts of  $H_2$  in the low temperature region compared with 0.001 mol% Pt/ $MoO_3$ . In the case of 0.01 mol% Pt/ $MoO_3$ , the amounts of  $H_2O$  formed in temperatures of 495–695 K were much larger than those of  $H_2$  consumed. Bond and Tripathi have reported that hydrogen bronzes of molybdenum begin to dehydrate at above 473 K.<sup>26,27</sup> Hence, temperature-programmed decomposition was conducted under an Ar flow using 0.01 mol% Pt/ $MoO_3$  heated to 423 K in a stream of 20%  $H_2$ –80% Ar. As shown in Fig. 6(c), the formation of  $H_2O$  was detected in the same temperature range as in the TPR, indicating that the formation of  $H_2O$  at temperatures of 495–695 K was caused by the decomposition of  $H_xMoO_3$ . In 0.001 mol% Pt/ $MoO_3$ , the formation and the decomposition of the  $H_xMoO_3$  phase seem to occur at almost the same time.

TPR profiles of Ru/ $MoO_3$  and  $MoO_3$  in a 20%  $H_2$ –80% Ar gas mixture are depicted in Fig. 7. 0.005 mol% Ru/ $MoO_3$  provided markedly different TPR profiles from those of Pt/ $MoO_3$ . 0.005 mol% Ru/ $MoO_3$  consumed negligible amounts

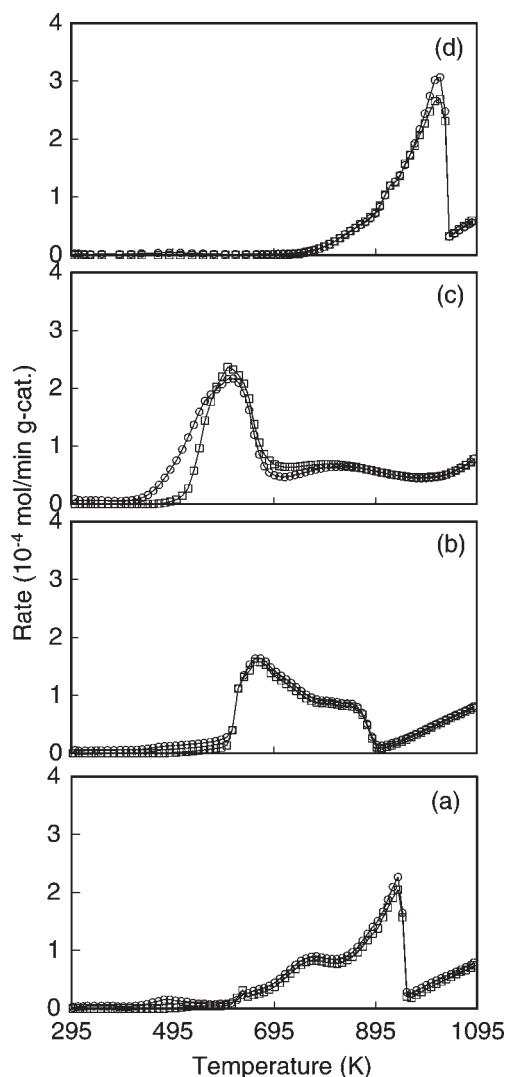


Fig. 7 TPR spectra of 0.005 mol% Ru/ $MoO_3$  (a), 0.01 mol% Ru/ $MoO_3$  (b), 0.1 mol% Ru/ $MoO_3$  (c) and  $MoO_3$  (d). Conditions: sample weight, 0.4 g; gas, 20%  $H_2$ –Ar; flow rate, 20 ml  $min^{-1}$ ; heating rate, 5 K  $min^{-1}$ ;  $H_2$  consumption ( $\circ$ ),  $H_2O$  formation ( $\square$ ).

of  $H_2$  at low temperatures, and the  $H_2$  consumption profile was analogous to the  $H_2O$  formation profile. The maximum peaks for  $H_2$  consumption and for  $H_2O$  formation appeared at 940 K. The peaks were shifted to lower temperature regions by loading of larger amounts of Ru. 0.1 mol% Ru/ $MoO_3$  exhibited almost the same TPR profile in the region of 695–1050 K as Pt/ $MoO_3$ , whereas it was difficult to evaluate the formation and decomposition of  $H_xMoO_3$  in 0.1 mol% Ru/ $MoO_3$  from the TPR. In  $MoO_3$ ,  $H_2$  consumption started at 752 K and the maximum  $H_2$  consumption peak was observed at 1023 K. The amounts of  $H_2$  consumed were consistent with those of  $H_2O$  formed. The consumed amount of  $H_2$  in the temperature range of 752–1050 K was  $6.4 \times 10^{-3}$  mol  $g^{-1}$ , which was equal to the amount of  $H_2$  required for reduction of  $MoO_3$  to  $MoO_2$ . The TPR profile of 0.005 mol% Ru/ $MoO_3$  in the high temperature regions was very similar to those of  $MoO_3$ . As shown in Figs. 2 and 3, 0.005 mol% Ru/ $MoO_3$  was converted to  $MoO_2$  during  $H_2$  reduction. Thus, the peak appearing at 940 K will reflect the formation of  $MoO_2$ . Since the  $MoO_2$  phase was detected by XRD in 0.01 mol% Ru/ $MoO_3$  after heating to 673 K and above in an  $H_2$  flow, the peaks for  $H_2$  consumption and  $H_2O$  formation at temperatures of 780–900 K seem to originate from reduction to  $MoO_2$ .

The amount of  $H_2$  reacted with 0.01 mol% Pt/ $MoO_3$  in 295–473 K was calculated to be  $6.2 \times 10^{-3}$  mol/ $g-MoO_3$  from the TPR spectrum shown in Fig. 6. This value can account for the formation of  $H_{1.68}MoO_3$ . As shown in Fig. 5, 0.001 mol% Pt/ $MoO_3$  was converted to  $H_{1.68}MoO_3$  at 473 K. However, the amount of  $H_2$  consumed in 298–473 K was evaluated to be  $1.7 \times 10^{-3}$  mol/ $g-MoO_3$  from the TPR spectrum. This discrepancy could be related to the difference in partial pressure of  $H_2$  because the XRD studies were performed using pure  $H_2$ , while a 20%  $H_2$ –80% Ar gas mixture was employed for the TPR studies. Hence, TPR was carried out using a 50%  $H_2$ –50% Ar gas mixture to study the effect of partial pressure of  $H_2$  on the reduction process.

Typical results are shown in Fig. 8. In the case of 0.001 mol% Pt/ $MoO_3$ , the TPR spectrum in the low temperature region varied with partial pressure of  $H_2$ , although the partial pressure of  $H_2$  showed no effect on the spectrum in the high temperature region. The amount of  $H_2$  consumed during heating from 298 to 473 K in 50%  $H_2$ –50% Ar was  $4.2 \times 10^{-3}$  mol/ $g-MoO_3$ , from which the value of  $x$  in  $H_xMoO_3$  was calculated to be 1.22. 0.1 mol% Ru/ $MoO_3$  gave the maximum peaks for  $H_2$  consumption and  $H_2O$  formation at 560 and 590 K, respectively, in 50%  $H_2$  atmosphere, while these peaks appeared at 615 K in 20%  $H_2$ –80% Ar. The formation of  $H_xMoO_3$  was promoted in 0.005 mol% Ru/ $MoO_3$  by an increase in partial pressure of  $H_2$ . However, the TPR profile of 0.005 mol% Ru/ $MoO_3$  differed markedly from the other catalysts even in 50%  $H_2$ –50% Ar. The peak for reduction to  $MoO_2$  appeared at 863 K. We propose from the results of XRD and TPR that reduction of 0.005 mol% and 0.01 mol% Ru/ $MoO_3$  is accompanied by the formation of both  $MoO_2$  and  $H_xMoO_3$ , probably due to its low activity for hydrogen activation, while 0.001–0.1 mol% Pt/ $MoO_3$  and 0.1 mol% Ru/ $MoO_3$  are reduced through the  $H_xMoO_3$  phases without the formation of  $MoO_2$ . Pt/ $MoO_3$  and 0.1 mol% Ru/ $MoO_3$  gave broad peaks in the temperature region of 695–1050 K. These peaks are considered to reflect the reduction to  $MoO_xH_y$ , because the  $MoO_xH_y$  phase was observed in XRD after the disappearance of  $H_xMoO_3$ .

As shown in Fig. 8, reduction to Mo metal started at 900 K in 0.005 mol% Ru/ $MoO_3$ , and at around 1050 K in 0.001 mol% Pt/ $MoO_3$  and 0.1 mol% Ru/ $MoO_3$ . These results indicate that reduction of  $MoO_2$  to Mo metal was faster than that of  $MoO_xH_y$  to Mo metal. As shown in Table 3, 0.005 mol% Ru/ $MoO_3$  exhibited a large reduction degree compared with other catalysts after reduction at 773 K for 12 h. This seems

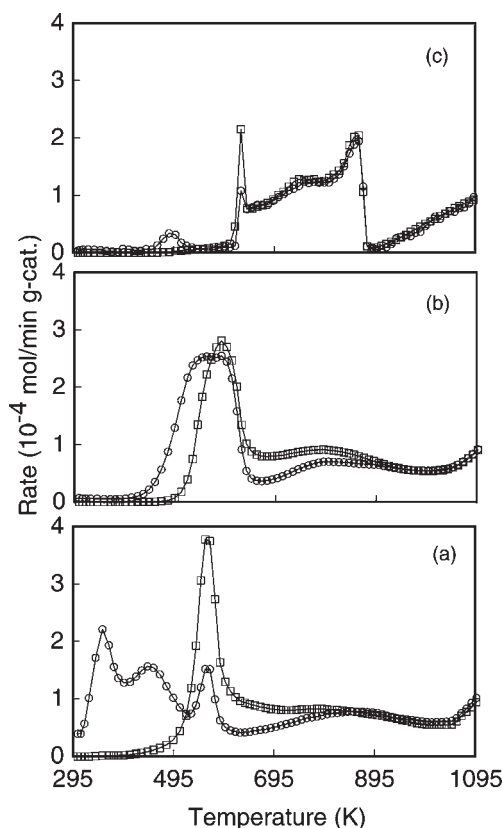


**Fig. 8** TPR spectra of 0.001 mol% Pt/MoO<sub>3</sub> (a), 0.1 mol% Ru/MoO<sub>3</sub> (b) and 0.005 mol% Ru/MoO<sub>3</sub> (c). Conditions: sample weight, 1 g; gas, 50% H<sub>2</sub>-Ar; flow rate, 20 ml min<sup>-1</sup>; heating rate, 5 K min<sup>-1</sup>; H<sub>2</sub> consumption (○), H<sub>2</sub>O formation (□).

to be attributed to the formation of MoO<sub>2</sub>, which can easily be reduced to Mo metal.

0.01 mol% Ru/MoO<sub>3</sub> had the lowest activities for pentane isomerization and for propan-2-ol dehydration among the catalysts with 0.01 mol% noble metal after reduction at 773 K for 12 h. The isomerization and the dehydration activities of H<sub>2</sub>-reduced Ru/MoO<sub>3</sub> was enlarged by an increase in the amount of Ru loading, whereas those of H<sub>2</sub>-reduced Pt/MoO<sub>3</sub> was independent of the amount of Pt. Reduction of Pt/MoO<sub>3</sub> proceeded *via* the H<sub>x</sub>MoO<sub>3</sub> phases, and yielded a MoO<sub>x</sub>H<sub>y</sub> phase, irrespective of the amount of Pt. By contrast, the reduction process of Ru/MoO<sub>3</sub> varied with the amount of Ru. The formation of the MoO<sub>2</sub> phase was suppressed and that of H<sub>x</sub>MoO<sub>3</sub> was enhanced by an increase in the amount of Ru. No appreciable difference appeared in XRD and TPR results between 0.01 mol% Pd/MoO<sub>3</sub> and 0.01 mol% Pt/MoO<sub>3</sub>. 0.01 mol% Rh/MoO<sub>3</sub> and 0.01 mol% Ir/MoO<sub>3</sub> gave similar XRD and TPR results to 0.1 mol% Ru/MoO<sub>3</sub>. We propose from these results that the low isomerization and dehydration activities of H<sub>2</sub>-reduced 0.005 and 0.01 mol% Ru/MoO<sub>3</sub> can result from its reduction process, which involves the formation of the MoO<sub>2</sub> phase.

Our previous papers<sup>12,18</sup> showed that reduction of MoO<sub>3</sub> at temperatures above 673 K did not yield the H<sub>x</sub>MoO<sub>3</sub> and MoO<sub>x</sub>H<sub>y</sub> phases at all. H<sub>2</sub>-Reduced MoO<sub>3</sub> with a reduction degree of about 80% was a mixture of MoO<sub>2</sub> and Mo metal, and had a surface area of 30–40 m<sup>2</sup> g<sup>-1</sup>. As shown in Figs. 2 and 3, 0.005 mol% Ru/MoO<sub>3</sub> was partly converted to H<sub>0.34</sub>MoO<sub>3</sub>, and then to MoO<sub>x</sub>H<sub>y</sub> during H<sub>2</sub> reduction. H<sub>2</sub>-Reduced 0.005 mol% Ru/MoO<sub>3</sub>, with a reduction degree of 82% consisted of MoO<sub>2</sub>, MoO<sub>x</sub>H<sub>y</sub>, and Mo metal phases, and its surface area was 152 m<sup>2</sup> g<sup>-1</sup>. Furthermore, H<sub>2</sub>-reduced 0.005 mol% Ru/MoO<sub>3</sub> was more active for the isomerization and the dehydration than H<sub>2</sub>-reduced MoO<sub>3</sub>. These results

also show that the physical and catalytic properties of MoO<sub>3</sub> will be improved by H<sub>2</sub> reduction involving the formation of H<sub>x</sub>MoO<sub>3</sub>, but not by reduction through MoO<sub>2</sub>. As the active catalysts for the pentane isomerization and the propan-2-ol dehydration contained the MoO<sub>x</sub>H<sub>y</sub> phase, the MoO<sub>x</sub>H<sub>y</sub> phase, which can originate from H<sub>x</sub>MoO<sub>3</sub> is likely to play an important role in the generation of the acidity.

## Conclusions

Reactions of pentane and propan-2-ol were carried out using H<sub>2</sub>-reduced MoO<sub>3</sub> with noble metals. There was no appreciable difference in the pentane isomerization activity and in the propan-2-ol dehydration activity among Pt, Pd, Rh and Ir/MoO<sub>3</sub> catalysts after reduction at 773 K for 12 h. The isomerization and dehydration activities of H<sub>2</sub>-reduced Ru/MoO<sub>3</sub> were lower than those of the other catalysts. The isomerization and the dehydration activities of H<sub>2</sub>-reduced Pt/MoO<sub>3</sub> varied very little with the amount of Pt. In the case of H<sub>2</sub>-reduced Ru/MoO<sub>3</sub>, however, the isomerization and dehydration activities were increased and the dehydrogenation activity was lowered by an increase in the amount of Ru. We conclude from these results that the isomerization activity of H<sub>2</sub>-reduced MoO<sub>3</sub> with noble metals can be determined by the ability to act as an acid catalyst. XRD and TPR studies showed that the reduction process of Ru/MoO<sub>3</sub> was affected by the amount of Ru. The formation of MoO<sub>2</sub> was suppressed and that of H<sub>x</sub>MoO<sub>3</sub> was promoted by an increase in the amount of Ru. By contrast, reduction of Pt/MoO<sub>3</sub> involved the formation of a hydrogen molybdenum bronze, H<sub>x</sub>MoO<sub>3</sub>, irrespective of the amount of Pt. We suggest from these results that the active phase for pentane isomerization and propan-2-ol dehydration can generate from reduction of H<sub>x</sub>MoO<sub>3</sub>.

## Acknowledgements

This work was supported in part by a Grant-in-Aid for Science Research (C) from the Japanese Society for the Promotion of Science.

## References

- 1 F. H. Ribeiro, R. A. Dalla Betta, M. Boudart, J. E. Baumgartner and E. Iglesia, *J. Catal.*, 1991, **130**, 86.
- 2 F. H. Ribeiro, M. Boudart, R. A. Dalla Betta and E. Iglesia, *J. Catal.*, 1991, **130**, 498.
- 3 E. Iglesia, J. E. Baumgartner, F. H. Ribeiro and M. Boudart, *J. Catal.*, 1991, **131**, 523.
- 4 E. Iglesia, F. H. Ribeiro, M. Boudart and J. E. Baumgartner, *Catal. Today*, 1992, **15**, 307.
- 5 E. A. Blekkam, C. Pham-Huu, M. J. Ledoux and J. Guille, *Ind. Eng. Chem. Res.*, 1994, **33**, 1657.
- 6 M. J. Ledoux, C. Pham-Huu, P. Delporte, E. A. Blekkam, A. P. E. York, E. G. Derouane and A. Fonseca, *Stud. Surf. Sci. Catal.*, 1994, **92**, 81.
- 7 C. Pham-Huu, P. D. Gallo, E. Peschiera and M. J. Ledoux, *Appl. Catal.*, 1995, **132**, 77.
- 8 A. P. E. York, C. Pham-Huu, P. D. Gallo, E. A. Blekkam and M. J. Ledoux, *Ind. Eng. Chem. Res.*, 1996, **35**, 672.
- 9 P. Delporte, F. Meunier, C. Pham-Huu, P. Vennegues, M. J. Ledoux and J. Guille, *Catal. Today*, 1995, **23**, 251.
- 10 C. Pham-Huu, A. P. E. York, M. Benaissa, P. D. Gallo and M. J. Ledoux, *Ind. Eng. Chem. Res.*, 1995, **34**, 1107.
- 11 T. Matsuda, H. Shiro, H. Sakagami and N. Takahashi, *Catal. Lett.*, 1997, **47**, 99.
- 12 T. Matsuda, Y. Hirata, H. Itoh, H. Sakagami and N. Takahashi, *Microporous Mesoporous Mater.*, 2000, **42**, 337.
- 13 T. Matsuda, Y. Hirata, H. Sakagami and N. Takahashi, *Microporous Mesoporous Mater.*, 2000, **42**, 345.
- 14 T. Matsuda, Y. Hirata, S. Suga, H. Sakagami and N. Takahashi, *Appl. Catal. A: Gen.*, 2000, **193**, 185.

- 15 A. Katrib, V. Logie, N. Saurel, P. Wehrer, H. Leflaive and G. Maire, *Surf. Sci.*, 1997, **377–379**, 754.
- 16 T. Matsuda, F. Uchijima, S. Endo and N. Takahashi, *Appl. Catal. A: Gen.*, 1999, **176**, 91.
- 17 F. Uchijima, T. Takagi, H. Itoh, T. Matsuda and N. Takahashi, *Phys. Chem. Chem. Phys.*, 2000, **2**, 1077.
- 18 T. Matsuda, F. Uchijima, H. Sakagami and N. Takahashi, *Phys. Chem. Chem. Phys.*, 2001, **3**, 4430.
- 19 T. Matsuda, A. Hanai, F. Uchijima, H. Sakagami and N. Takahashi, *Microporous Mesoporous Mater.*, 2002, **51**, 155.
- 20 T. Matsuda, Y. Hirata, M. Suzuki, H. Sakagami and N. Takahashi, *Chem. Lett.*, 1999, **9**, 873.
- 21 T. Matsuda, Y. Hirata, F. Uchijima, H. Itoh and N. Takahashi, *Bull. Chem. Soc. Jpn.*, 2000, **73**, 1029.
- 22 T. Matsuda, A. Hanai, F. Uchijima, H. Sakagami and N. Takahashi, *Bull. Chem. Soc. Jpn.*, 2002, **75**, 1165.
- 23 F. C. Meunier, *Chem. Commun.*, 2003, 1954.
- 24 T. Matsuda, K. Watanabe, H. Sakagami and N. Takahashi, *Appl. Catal. A: Gen.*, 2003, **242**, 267.
- 25 T. Matsuda, H. Kodama, H. Sakagami and N. Takahashi, *Appl. Catal. A: Gen.*, 2003, **248**, 269.
- 26 G. C. Bond and J. B. Tripathi, *J. Chem. Soc., Faraday Trans. I*, 1976, **72**, 933.
- 27 G. C. Bond and J. B. Tripathi, *J. Less-Common Met.*, 1974, **36**, 31.